


190-mJ cryogenically-cooled Yb:YLF amplifier system at 1019.7 nm

HUSEYIN CANKAYA,^{1,2,3,*}  UMIT DEMIRBAS,^{1,4}  YI HUA,^{1,2}
MICHAEL HEMMER,¹  LUIS E. ZAPATA,¹ MIKHAIL PERGAMENT,¹
AND FRANZ X. KAERTNER^{1,2,3} 

¹Center for Free-Electron Laser Science, Deutsches Elektronen-Synchrotron DESY, Notkestraße 85, 22607 Hamburg, Germany

²Physics Department, University of Hamburg, Luruper Chaussee 149, 22761 Hamburg, Germany

³The Hamburg Centre for Ultrafast Imaging, Luruper Chaussee 149, 22761 Hamburg, Germany

⁴Laser Technology Laboratory, Antalya Bilim University, 07190 Dosemealti, Antalya, Turkey

*huseyin.cankaya@cfel.de

Abstract: We report 190-mJ pulses with spectral content supporting sub-ps pulse-duration at a 10 Hz repetition rate generated by a cryogenically-cooled, bulk Yb:YLF laser amplifier system. The amplifier system relies on a chirped pulse amplification architecture and consists of a fiber front-end, a regenerative amplifier, and two 4-pass amplifiers. The fiber front-end delivers 15-nJ, 1-ns stretched seed pulses, which are first amplified to 13-mJ pulse energy inside a Yb:YLF regenerative amplifier. Then the pulses are boosted further to 115 mJ and 190 mJ in two consecutive 4-pass amplifiers. To our knowledge, these are the highest pulse energies reported from Yb:YLF based amplifiers to date. We foresee shortening the pulsewidths to sub-400-fs range in future studies.

© 2019 Optical Society of America under the terms of the [OSA Open Access Publishing Agreement](#)

1. Introduction

Yb:YAG is a very attractive laser gain material for high-average power laser oscillators and amplifiers in rod [1,2], crystal fiber [3] and thin-disk geometries [4–7] due to its long fluorescence lifetime, and large emission cross-section. When Yb:YAG is cooled to cryogenic temperatures, it becomes a four-level laser gain medium with improved thermo-mechanical properties [8–10] allowing efficient amplification [1,2,11]. However, the gain bandwidth of Yb:YAG narrows down significantly at cryogenic temperatures and limits the attainable pulsewidth to a few picoseconds. Alternatively, Yb:YLF possess very broad, and smooth gain profile (bandwidth spanning 10 nm for the E//a axis) at cryogenic temperatures [12], enabling broadband amplification with reduced gain narrowing effects with respect to Yb:YAG. The relatively large emission bandwidth in cryogenic Yb:YLF comes at the expense of a reduced emission cross-section, yielding low small-signal gain and high saturation fluence as compared to Yb:YAG which places the saturation fluence well above the damage threshold for stretched pulse durations reasonably achievable in a CPA architecture.

Previously, several groups reported cryogenically-cooled Yb:YLF laser oscillators and amplifiers. In the continuous-wave regime, output powers up to 224 W and a slope efficiency approaching 70% have been demonstrated at 995 nm wavelength [13]. In Q-switched operation, 60-ns pulses around 995 nm at 10 kHz repetition rate with an average power of 50 W was demonstrated with a similar slope efficiency [14]. In the chirped-pulse amplifier regime, Rand et al. reported 1-mJ pulses supporting sub-900 fs pulses at 10 kHz from a regenerative amplifier [12]. By using this regenerative amplifier output as the seed for an 8-pass amplifier, Miller et al. demonstrated 10-mJ pulses with 865 fs pulse duration at 10 kHz repetition rate, corresponding to 100 W of average power [15]. In the high-energy, low-repetition rate operation regime, Kawanaka et al. demonstrated a regenerative amplifier producing 30-mJ pulses with 800 fs pulse duration at

20 Hz [16]. Later, Ogawa improved the amplified pulse energy to 107 mJ by pumping harder with several diode modules in a similar amplifier scheme [17].

In this work, we demonstrate 190-mJ pulses from a three-stage cryogenically cooled Yb:YLF amplifier system at 10 Hz repetition rate. This is the highest reported pulse energy from a cryogenically-cooled Yb:YLF amplifier system. The amplified spectrum supports sub-ps pulses centered around 1019.7 nm.

2. Experimental setup

Figure 1 shows the simplified block diagram of the experimental setup consisting of a fiber front-end, a regenerative amplifier, two 4-pass amplifiers along with the layout of the two 4-pass amplifiers. Details of the 4-pass amplifiers, that feature similar architectures, is also shown as an inset. The fiber front-end delivers 15-nJ seed-pulses at 38 MHz stretched to 1 ns full-width half-maximum (FWHM) pulse duration by using fiber Bragg gratings with a stretching ratio of ~ 400 ps/nm. The details of the fiber front-end are given in [18]. The stretched pulses are first amplified to the 13 mJ pulse energy level inside the cryogenically-cooled Yb:YLF regenerative amplifier system at 10 Hz. The regenerative amplifier consists of a 4-mirror bowtie ring geometry. Inside the cavity, a 1.75 -mm long, 25%-doped Yb:YLF gain medium is pumped by a 960 nm diode laser delivering up to 280 W continuous-wave pump power. This pump diode is however operated in the quasi-CW regime at a 2% duty cycle. The crystal is mounted on a copper heat sink attached to a liquid nitrogen dewar and cooled down to 77 K. The experimental details of the regenerative amplifier setup are described in [19].

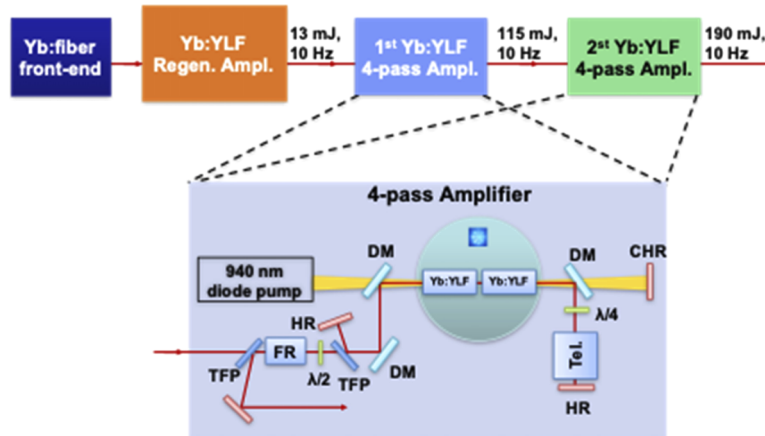


Fig. 1. Schematic of the cryogenically cooled Yb:YLF amplifier system consisting of an Yb: fiber front-end, a regenerative amplifier, and two 4-pass amplifiers. The layout of the two 4-pass amplifiers is illustrated in more details. FR, $\lambda/2$, TFP, HR, CHR, DM, $\lambda/4$, Tel. stand for Faraday rotator, a half-wave plate, thin-film polarizer, high-reflector, curved high-reflector, dichroic mirror, quarter wave-plate, and telescope; respectively. In the first 4-pass amplifier, the 0.5% Yb doped, 25-mm long YLF crystal is pumped from both sides by recycling the unabsorbed pump light. In the second 4-pass amplifier, CHR is replaced by a beam block to avoid recycling of the pump beam. Both amplifiers are pumped at 940 nm.

The beam at the output of the regenerative amplifier is upsized to 4-mm diameter at $1/e^2$ and coupled into the injection line of the first 4-pass amplifier which consists of a thin-film polarizer (TFP), a 12 mm aperture Faraday rotator (FR), a half-wave plate ($\lambda/2$), a second TFP and two dichroic mirrors (DMs) in consecutive order. The seed pulses pass 4 times through two Yb:YLF crystals in series attached to a common copper heat sink cooled down to 77 K via boiling liquid

nitrogen. The 20-mm-long Yb:YLF crystals with an aperture of 10×15 mm have 0.5% doping concentration and 3-mm undoped caps on both sides to minimize surface deformations. Both crystals are kept under vacuum with a pressure less than 10^{-6} mbar at 77 K. E//a-axis of the crystals were employed in amplification. The polarization of the seed pulse is switched between s and p-polarization by using a quarter-wave plate ($\lambda/4$) in double-pass geometry, after the first and third passes through the gain media. The thermal and population lensing originated inside gain media is compensated by employing a two-lens telescope after the first and third passes. The amplifier crystals are pumped by a diode laser module providing up to 2 kW continuous-wave power at 940 nm. The pump beam is delivered into the crystals via a fiber with a core diameter of 600 μm (NA 0.2) coupled out with a telescope resizing the beam to flat-top 4-mm size. To avoid undesired thermal issues due to high-average power, the diode laser is gated to deliver pump pulses at 10 Hz with 4-ms pulse duration. For the first 4-pass amplifier, the unabsorbed pump beam (20% of the incident power) is separated with a DM and recycled to pump the gain medium once more. The recycled pump beam is coupled back to the gain media by using a curved mirror imaging the pump beam into the crystals slightly off to avoid feedback to the pump diode laser.

The second 4-pass amplifier has the same architecture as the first 4-pass amplifier but different beam parameters to circumvent the laser-induced damage on the optics. The beam at the output of the first 4-pass amplifier is collimated and resized to 5.5-mm beam diameter at $1/e^2$ and coupled into the second 4-pass amplifier. During the amplification, the beam size is controlled by adjusting the distance between the telescope lenses inside the amplifier. The flat-top diode pump laser beam having 4.1 mm beam diameter is imaged into gain media. The pump and the seed beam sizes are intentionally mismatched to reduce the effect of the gain shaping at the expense reduced efficiency in the amplifier. Gain shaping is a significant effect, where the center of the Gaussian beam experiences more gain than the tail which leads to a decrease of the beam-size inside the gain medium for an unsaturated amplifier system like Yb:YLF. In the second 4-pass amplifier, the unabsorbed pump is not recycled because the amplification is mainly limited by the damage to the optics.

To demonstrate the compressibility of the amplified pulses, the output of the first 4-pass amplifier is coupled into a Treacy compressor which consists of two gold-coated gratings with groove density of 1740 lines/mm. The perpendicular grating separation is adjusted to ~ 91 cm for optimum compression.

3. Results and discussion

Figure 2(a) shows the spectra of the pulses from the fiber front-end and the regenerative amplifier (Regen.). As can be seen, both spectra are centered around 1019.7 nm with spectral bandwidth (FWHM) of 2.3 nm hence there is no significant gain narrowing effect due to relatively flat gain spectrum of Yb:YLF gain medium at cryogenic temperatures. The amplified spectrum from the regenerative amplifier supports pulses less than 650 fs. The bandwidth of the amplified pulses is mainly limited by the current fiber front-end. As can be seen from the emission cross-section measurement in Fig. 2(a), Yb:YLF has a very flat gain profile between 1015 and 1020 nm which enables broadband amplification supporting less than 400 fs. The bandwidth of the amplified pulses can be improved further by employing a seed source having a broader spectrum than currently available with the same stretched pulse duration without changing the architecture of the amplifier system.

The regenerative amplifier can amplify the seed pulse from 15 nJ up to 13 mJ at 10 Hz [19]. Figure 2(b) shows the pulse energy stability of the amplified pulses delivered by the regenerative amplifier over 4 hours, for every pulse without any averaging or subsampling. The regenerative amplifier exhibits 1.3% pulse energy stability with 10.55-mJ average pulse energy under moderate pumping level. Within the first 2-hours, the pulse energy measurement shows slight oscillation

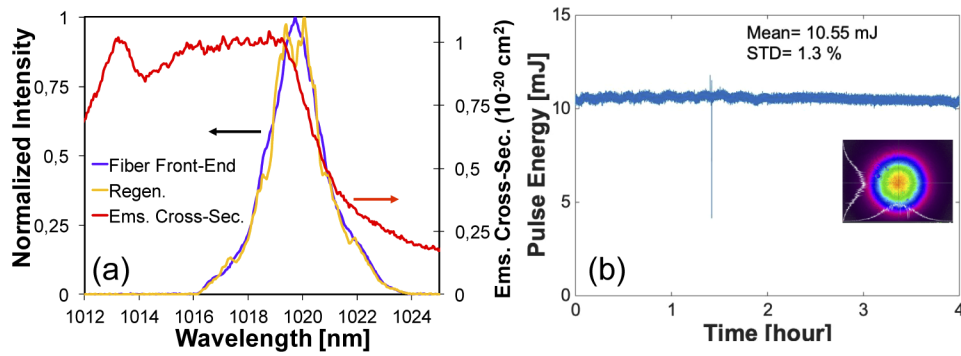


Fig. 2. (a) Spectra of the fiber front-end and regenerative amplifier (regen.) and emission cross-section of Yb:YLF for the electric field plane parallel to a-axis at 80 K. (b) Pulse energy measurement of the regenerative amplifier over 4 hours and near field beam profile at the output of the regenerative amplifier (inset).

which is due to the temperature variations of the cooling water of the diode laser hence the slight shift in laser diode wavelength, resulting in absorption variation in the regenerative amplifier. After a two-hour operation, the temperature of the diode settles to the equilibrium temperature. Furthermore, the regenerative amplifier produces a beam having nearly Gaussian beam profile in the near-field (inset Fig. 2(b)).

Figure 3(a) shows the output pulse energy measurements for the two 4-pass amplifiers as a function of pump fluence. All the pulse energies are recorded for the telescope configuration which is compensating the thermal and population lensing at the highest pump power. For the first 4-pass amplifier, the amplified pulse energy measurement is demonstrated for two cases, where the unabsorbed pump is dumped (1-side) and recycled (2-side) by imaging the unabsorbed pump into the crystals again. In the case of 1-side pumping, the first 4-pass amplifier boosted up the energy of the pulses from 13 mJ to 99 mJ. With the implementation of the 2-side pumping, the amplification is improved to 140-mJ pulse energy under pump fluence of 64 J/cm^2 . The fluence inside the gain media is estimated to be 2.24 J/cm^2 for 140 mJ output pulses where the damage threshold of the optics is above 3.16 J/cm^2 for 1 ns pulses. The single-pass loss of the first 4-pass amplifier – when the crystal is at cryogenic temperature – is measured to be $\sim 4\%$. Figure 3(b) demonstrates the pulse energy stability of the first 4-pass amplifier at 96.9 mJ over ~ 4 hours, the near and far-field image of the beam profile (insets). Pulse to pulse energy fluctuation is measured to be 3.5% .

The second 4-pass amplifier is pumped only from one-side due to the limitation of the damage threshold of the optics for the amplified pulses. When 115-mJ pulses from the first 4-pass amplifier are injected into the second 4-pass amplifier, it can deliver 190-mJ pulses at 10 Hz with very good beam profile in near and far-field (Fig. 3(a) – insets). The fluence inside the second 4-pass amplifier is as high as 2.88 J/cm^2 which is close to the damage threshold of our optics inside the amplifier (10 J/cm^2 for 10-ns pulses corresponds to 3.16 J/cm^2 for 1 ns pulses). We observed damage on the Anti-Reflection (AR) coating of our chamber windows after a few-minutes operation which has the lowest damage threshold. This can be improved by replacing those windows by the ones with the AR coatings based on an ion-beam sputtering technique which provides coatings with relatively higher damage threshold ($\sim 7 \text{ J/cm}^2$ for 1 ns pulses). The second 4-pass amplifier can be operated safely at 165-mJ energy level on the long-term, even with the low-damage threshold windows. The single-pass loss of the second amplifier is $\sim 9\%$ which is higher than the first 4-pass. The main contribution to the loss is non-optimum AR coatings of the chamber windows which can be improved by replacing them with optimum ones resulting in

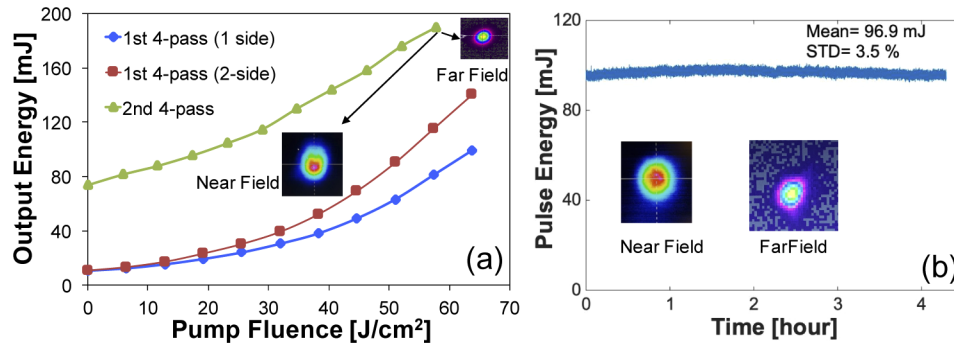


Fig. 3. (a) Pulse energy measurement with respect to pump fluence for the 4-pass amplifiers and near and far-field beam profiles of the second 4-pass amplifier with 190-mJ output pulse energy (insets). (b) Pulse energy measurement of the first 4-pass amplifier over ~4 hours, near and far-field image of the beam profile (insets).

higher extraction efficiency from the amplifier. As a consequence of low repetition rate operation, the optical-to-optical conversion efficiencies of the first and second 4-pass amplifiers are quite low as expected, at 1.8 and 2.4%, respectively. The efficiencies are mainly limited by the number of passes through the gain media and the damage threshold of the material which is lower than the saturation fluence of Yb:YLF gain medium. The efficiencies could be slightly improved by increasing the number of passes through the gain medium via employment of other amplifier architectures. For a more significant improvement, an increase in the repetition rate over the limit of the inverse of the upper laser level fluorescence lifetime (over 500 Hz) would reduce the effective saturation fluence via cumulative extraction of pulses. This would allow one to reach the saturation before damaging the crystal which could result in significant enhancement in extraction and the optical-to-optical conversion efficiency. On the other hand, the increase in repetition rate will be limited by the maximum achievable average output power from the system (100–300 W for single crystal, due to limited cooling capability in rod geometry).

Figure 4(a) shows the spectra of the two 4-pass amplifiers at 90 mJ and 190 mJ pulse energies for the first and the second 4-pass amplifiers, respectively. Both spectra show a spectral bandwidth of 2.2 (FWHM) which supports pulses with ~650 fs (FWHM) duration (Fig. 4(b) inset). As can be seen, there is no significant gain narrowing due to the flat gain spectrum of the Yb:YLF amplifier system. To demonstrate the compressibility of the amplified pulses, we coupled 90-mJ pulses from the output of the first 4-pass amplifier into a Treacy grating compressor. Figure 4(b) shows the second harmonic background-free auto-correlation trace of the compressed pulses. As can be seen, the auto-correlation trace has 2.1 ps (FWHM) duration which corresponds to 1.35 ps pulse duration with the assumption of sech^2 pulse shape. The discrepancy between the transform-limited pulse duration and the measured one is due to the dispersion mismatch between the chirped fiber Bragg gratings and the grating compressor. The B-integral in the amplifier system is kept below 1 to avoid any nonlinear contribution to the dispersion management. As mentioned before the Yb:YLF amplifier system supports significantly broader spectral bandwidth (>4 nm) for this particular polarization state. In the next step, we are planning to replace the fiber-front-end including the fiber Bragg gratings with a broader bandwidth versions and optimize the dispersion management such that we can compress the amplified pulses below 400 fs without changing the amplifier architecture.

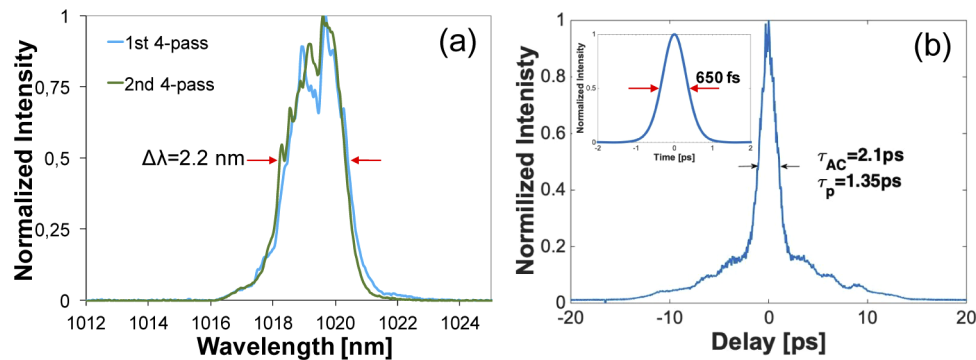


Fig. 4. (a) Spectra of the first (1st 4-pass) and the second four pass amplifiers (2nd 4-pass) (b) Auto-correlation trace of the compressed pulses from the first 4-pass amplifier and transform-limited pulse duration (inset).

4. Summary

In conclusion, we reported a cryogenically-cooled Yb:YLF amplifier system delivering 190-mJ pulses. The amplifier system relies on the chirped pulse amplification architecture and consists of a fiber-front end, a regenerative amplifier and two 4-pass amplifiers. This is the highest pulse energy reported from a Yb:YLF amplifier system to date. The amplified pulses show 2.2 nm (FWHM) bandwidth centered at 1019.7 nm and supporting ~650 fs long pulses with a Gaussian beam profile. Further shortening of the pulses could be achieved by improving the spectral bandwidth of the seed source to match the flat gain bandwidth of the Yb:YLF amplifier system which supports pulses below 400 fs.

Funding

European Research Council (609920); Deutsche Forschungsgemeinschaft (390715994).

Acknowledgment

The authors gratefully acknowledge the support of the engineering group, Thomas Tilp, Andrej Berg and Jelto Thesinga and the DESY vacuum group. The authors also thank Tobias Kroh and Felix Ritzkowski for implementing the long-term diagnostic tools. Finally, we would like to thank Kelly Zapata for implementing the metallization and indium bonding steps involved in the in-house mounting of these laser crystals. Dr. Demirbas acknowledges support from BAGEP Award of the Bilim Akademisi.

Disclosures

The authors declare no conflicts of interest.

References

1. L. E. Zapata, F. Reichert, M. Hemmer, and F. X. Kärtner, "250 W average power, 100 kHz repetition rate cryogenic Yb:YAG amplifier for OPCPA pumping," *Opt. Lett.* **41**(3), 492–495 (2016).
2. K.-H. Hong, C.-J. Lai, A. Siddiqui, and F. X. Kärtner, "130-W picosecond green laser based on a frequency-doubled hybrid cryogenic Yb:YAG amplifier," *Opt. Express* **17**(19), 16911–16919 (2009).
3. X. Délen, Y. Zaouter, I. Martial, N. Aubry, J. Didierjean, C. Hönninger, E. Mottay, F. Balembois, and P. Georges, "Yb:YAG single crystal fiber power amplifier for femtosecond sources," *Opt. Lett.* **38**(2), 109–111 (2013).
4. A. Giesen, H. Hügel, A. Voss, K. Wittig, U. Brauch, and H. OPOWER, "Scalable concept for diode-pumped high-power solid-state lasers," *Appl. Phys. B* **58**(5), 365–372 (1994).

5. A. Giesen and J. Speiser, "Fifteen Years of Work on Thin-Disk Lasers: Results and Scaling Laws," *IEEE J. Sel. Top. Quantum Electron.* **13**(3), 598–609 (2007).
6. J. Brons, V. Pervak, D. Bauer, D. Sutter, O. Pronin, and F. Krausz, "Powerful 100-fs-scale Kerr-lens mode-locked thin-disk oscillator," *Opt. Lett.* **41**(15), 3567–3570 (2016).
7. T. Nubbemeyer, M. Kaumanns, M. Ueffing, M. Gorjan, A. Alismail, H. Fattahi, J. Brons, O. Pronin, H. G. Barros, Z. Major, T. Metzger, D. Sutter, and F. Krausz, "1 kW, 200 mJ picosecond thin-disk laser system," *Opt. Lett.* **42**(7), 1381–1384 (2017).
8. R. L. Aggarwala, D. J. Ripin, J. R. Ochoa, and T. Y. Fan, "Measurement of thermo-optic properties of $\text{Y}_3\text{Al}_5\text{O}_{12}$, $\text{Lu}_3\text{Al}_5\text{O}_{12}$, YAlO_3 , LiYF_4 , LiLuF_4 , BaY_2F_8 , $\text{KGd}(\text{WO}_4)_2$, and $\text{KY}(\text{WO}_4)_2$ laser crystals in the 80–300 K temperature range," *J. Appl. Phys.* **98**(10), 103514 (2005).
9. T. Y. Fan, D. J. Ripin, R. L. Aggarwal, J. R. Ochoa, B. Chann, M. Tilleman, and J. Spitzberg, "Cryogenic Yb^{3+} -Doped Solid-State Lasers," *IEEE J. Sel. Top. Quantum Electron.* **13**(3), 448–459 (2007).
10. D. C. Brown, "The promise of cryogenic solid-state lasers," *IEEE J. Sel. Top. Quantum Electron.* **11**(3), 587–599 (2005).
11. L. E. Zapata, H. Lin, A.-L. Calendron, H. Cankaya, M. Hemmer, F. Reichert, W. R. Huang, E. Granados, K. H. Hong, and F. X. Kärtner, "Cryogenic Yb:YAG composite-thin-disk for high energy and average power amplifiers," *Opt. Lett.* **40**(11), 2610–2613 (2015).
12. D. Rand, D. Miller, D. J. Ripin, and T. Y. Fan, "Cryogenic Yb^{3+} -doped materials for pulsed solid-state laser applications [Invited]," *Opt. Mater. Express* **1**(3), 434–450 (2011).
13. L. E. Zapata, D. J. Ripin, and T. Y. Fan, "Power scaling of cryogenic Yb:LiYF₄ lasers," *Opt. Lett.* **35**(11), 1854–1856 (2010).
14. N. Ter-Gabrielan, V. Fromzel, T. Sanamyan, and M. Dubinskii, "Highly-efficient Q-switched Yb:YLF laser at 995 nm with a second harmonic conversion," *Opt. Mater. Express* **7**(7), 2396–2403 (2017).
15. D. E. Miller, L. E. Zapata, D. J. Ripin, and T. Y. Fan, "Sub-picosecond pulses at 100 W average power from a Yb:YLF chirped-pulse amplification system," *Opt. Lett.* **37**(13), 2700–2702 (2012).
16. J. Kawanaka, K. Yamakawa, H. Nishioka, and K.-I. Ueda, "30-mJ, diode-pumped, chirped-pulse Yb:YLF regenerative amplifier," *Opt. Lett.* **28**(21), 2121–2123 (2003).
17. K. Ogawa, Y. Akahane, and K. Yamakawa, in *CLEO: 2011 - Laser Science to Photonic Applications*, (2011), 1–2.
18. Y. Hua, W. Liu, M. Hemmer, L. E. Zapata, G. Zhou, D. N. Schimpf, T. Eidam, J. Limpert, A. Tünnermann, F. X. Kärtner, and G. Chang, "87-W 1018-nm Yb-fiber ultrafast seeding source for cryogenic Yb: yttrium lithium fluoride amplifier," *Opt. Lett.* **43**(8), 1686–1689 (2018).
19. M. Hemmer, L. E. Zapata, Y. Hua, and F. X. Kärtner, in *Lasers Congress 2016 (ASSL, LSC, LAC)*, OSA Technical Digest (online) (Optical Society of America, 2016), AT4A.3.